J Sol-Gel Sci Technol (2017) 83:197–206
DOI 10.1007/s10971-017-4378-z

ORIGINAL PAPER: SOL-GEL AND HYBRID MATERIALS WITH SURFACE MODIFICATION FOR APPLICATIONS

Preparation and properties of monolithic and hydrophobic gelatin–silica composite aerogels for oil absorption

Li Yun[1,2] · Jin Zhao[1,2] · Xiaoling Kang[1,2] · Yang Du[1,2] · Xubo Yuan[1,2] · Xin Hou[1,2]

Received: 2 October 2016 / Accepted: 28 March 2017 / Published online: 11 April 2017

Abstract In this study, highly porous and low density silica–gelatin composite aerogels with excellent absorption capacity were obtained. The preparation process was as follows: firstly, the gel with stable network structure was formed by sol–gel method; secondly, after soaking the gel with hexamethyldisilazane solution, the aerogel was prepared by freeze-drying; finally, the aerogel was coated with hexamethyldisilazane via chemical vapor deposition. The composite aerogels with 30% gelatin showed optimal performance in practical applications: lowest bulk density (0.068 g/cm^3), highest porosity (96%), largest pore volume (1.24 cm^3/g), and maximum oil/organic solvents absorption capacity (12–27 *g*/*g*). The excellent oil/solvent absorption capacity and recyclability indicated that the hydrophobic gelatin–silica composite aerogels could be a promising candidate for oil absorption.

Graphical Abstract

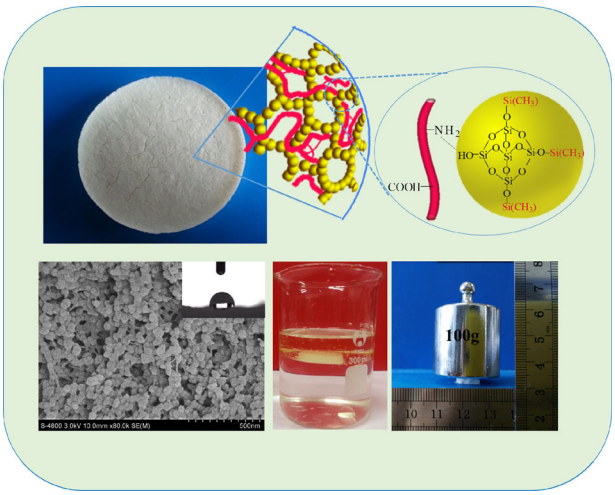

Keywords Gelatin · Silica aerogel · Composite · Hydrophobic · Porous structure · Oil absorption

1 Introduction

Oil spills or oil-contaminated waste water treatment has been a challenging issue and received widespread attention [1–4]. The present methods include in situ burning of oil spills, chemical dispersion using dispersing agents, biological degradation and physical absorption using absorbing materials. Among these methods, physical absorption based on absorbents is considered to be attractive, because the oil could be treated properly and the absorbents could be reused for several cycles. There are three classes of

Electronic supplementary material The online version of this article (doi:10.1007/s10971-017-4378-z) contains supplementary material, which is available to authorized users.

✉ Jin Zhao
zhaojin@tju.edu.cn

✉ Xin Hou
houxin@tju.edu.cn

[1] Tianjin Key Laboratory of Composite and Functional Materials, Tianjin University, Tianjin 300350, China

[2] School of Materials Science and Engineering, Tianjin University, Tianjin 300350, China

sorbents: natural organic sorbents, inorganic sorbents and synthetic organic sorbents. Natural organic sorbents such as cotton and straw possess low oil absorption capacity and hydrophility [5, 6]. Inorganic sorbents such as clay and zeolite exhibit poor floatability and slow kinetics [7]. Synthetic organic sorbents are non-biodegraded in spite of better oil absorption capacity [8, 9]. Therefore, it is desirable to search for a lightweight and biodegradable sorbent with high absorption capacity.

Silica aerogels, prepared by sol-gel method following by supercritical drying, and ambient pressure drying or freeze drying, are reported to be promising materials as lightweight oil adsorbing materials [1, 10–13], due to their exceptional properties, such as low density, large specific surface area, high porosity, and tailorable hydrophobicity. For example, Parale et al. [14] used trimethylchlorosilane as a precursor and ambient pressure drying as the drying method to synthesize silica aerogel with an oil absorbency of 14 *g/g*. In spite of the fascinating properties of silica aerogel, it is hard to be commercialized because of the inherent fragility. A pure silica aerogel with density of 0.12 g/cm^3 would be broken under the stress of 31 kPa [15]. However, the flexibility of organic materials makes them highly interesting in reducing the brittleness of inorganic aerogels. [16–19] Hence, incorporating organic materials into silica aerogels to form organic/inorganic hybrid aerogels would improve the mechanical properties, and promote practical application of silica aerogel in the field of oil absorption.

Strengthening the silica aerogels with polymers, including synthetic and natural polymers, could improve the mechanical property effectively. Common strategies included: (i) formation of physical or chemical bonding between polymers and hydroxyl groups on the silica gel surface. (ii) surface functionalization of native silica aerogels with functionalized trialkoxysilanes which react then with polymers. These methods extend the application of silica aerogels in the field of oil absorption [20–24]. For examples, resorcinol–formaldehyde-reinforced silica aerogel (Young's modulus was 8.15 MPa with density of 0.18 g/cm^3) prepared by Yun et al. could absorb 5.2 to 6.5 times of its own weight of organic liquid [25]. The flexible bacterial cellulose–silica composite aerogels could collect oil from water [26]. Compared with synthetic polymers, silica-based aerogels reinforced by the natural polymers as oil sorbents were more fascinating due to the abundant sources, low costs and biodegradability of natural polymers. However, the study on silica-based aerogels reinforced by natural polymers as oil sorbents were less reported.

In this study, hydrophobic porous silica-based aerogels reinforced with gelatin for oil absorption were prepared. Gelatin, as a kind of denatured polypeptide macromolecule, was extracted from skins, bones and connective tissue of animals and was of great importance in various fields such as food, pharmaceutical and medical industry [27–29]. Abundant amino and carboxyl groups in gelatin offered numerous chemical and physical cross-linking, functionalization and reactive sites. Thus it was a desirable material to form biodegradable composites with siloxane by simple sol–gel process [30–33]. Preparing porous gelatin–silica hybrid materials with applicable mechanical properties would extend practical values of silica aerogels in the fields of thermal insulation, drug delivery and tissue engineering [32, 34–38]. For instance, the hybrid magnetic scaffolds of gelatin–siloxane [37] were effective in stimulating cell growth and osteogenic differentiation, and thus the magnetic hybrid scaffolds may be useful for bone tissue engineering. However, fewer efforts were made on silica-gelatin aerogels used as oil sorbents. Here, the effects of gelatin on mechanical properties, oil/organic solvents absorption capacity, and absorption and desorption kinetics of silica aerogels were investigated.

2 Experiments

2.1 Materials

Tetraethoxysilane (TEOS; 99%) was used as silicon source precursor to form the silica backbones of the aerogels. Ethanol (EtOH), *n*-hexane, toluene, xylene, methylbenzene, dichloromethane, butyl acetate, acetone, and pentane were used as solvents. They were purchased from Tianjin Jiangtian Chemical Reagent Co., Ltd. (Tianjin, China). Gelatin (>99%) was provided by Beijing Yinfeng Century Technology Development Co., Ltd. (Beijing, China). Oxalic acid (>99.5%) as pH regulator and hexamethyldisilazane (HDMZ; analytical grade) as hydrophobic modifier were from Tianjin Kemiou Chemical Reagent Co., Ltd. (Tianjin, China). Gasoline and arachis oil were bought from market.

2.2 Preparation of gelatin–silica composite aerogel

One-step sol-gel method was carried out using gelatin and TEOS as co-precursors. A certain amount of gelatin was dissolved in 30 ml deionized (DI) water. Then this fully dissolved gelatin solution was mixed with 5 mL TEOS and oxalic acid (0.1 mol/L) solution was added dropwise to adjust pH to 3–4 under magnetic stirring for 10–12 h at 30 °C. The sols were poured into polystyrene-cultivating disks and aged for 48 h for stable networks formation. Afterwards, the gel was washed with DI water for several times and dried in a vacuum freeze drying apparatus (SCIENTZ-12). The samples of the gelatin-silica composite aerogels were marked as 0-gs, 10-gs, 20-gs, 30-gs, 40-gs,

Table 1 Porous properties of hydrophobic gelatin–silica composite aerogels

Sample	Gelatin (g)	TEOS (ml)	Bulk density (g/cm^3)	Porosity (%)	Pore volume (cm^3/g)
0-GS	0	5	0.168	91	0.72
10-GS	0.1488	5	0.132	92	0.88
20-GS	0.3350	5	0.090	94	1.02
30-GS	0.5740	5	0.068	96	1.24
40-GS	0.8928	5	0.096	91	1.12

where the numbers represented the mass fraction of gelatin in the composite aerogels.

A series of hydrophobic gelatin–silica composite aerogels with different mass percentage gelatin (Table 1) were prepared. HDMZ was used as hydrophobic modifier. The wet composite gel obtained through the above mentioned process was immersed in a 10 vol % HDMZ–hexane solution, and then the modified wet gel was washed with hexane, EtOH and DI water for 24 h successively and dried in vacuum freeze drying apparatus. Finally, the resultant composite aerogel was placed in a sealed glass dish containing HDMZ at 50 °C for several hours to ensure the complete modification of the surface. The samples and formula were presented in Table 1. For example, 20-GS represented the hydrophobic gelatin–silica composite aerogel in which the mass ratio of silicon to gelatin was 20%.

2.3 Characterizations and tests

2.3.1 Chemical structure characterization

Fourier transform infrared spectroscopy (FTIR) with 4 cm^{-1} resolution was employed to confirm the chemical structure of aerogels (Bruker Tensor 27). The samples were mixed with KBr at the mass ratio of 1:100 and pressed into pellets. The scan number was 16. The scanning range was 4000–400 cm^{-1}.

2.3.2 Morphology

The microstructure of aerogel was observed using field emission scanning electron microscopy (Hitachi S4800) with an acceleration voltage of 5 kV. The specimens were sputter-coated with Au for 50 s before SEM measurement.

2.3.3 Thermostabiliy

Thermogravimetric (TG) analysis was measured with Netzsch TG 209 under nitrogen atmosphere. The temperature ranges from 20 to 800 °C at a heating rate of 10 °C/min.

2.3.4 The water contact angle tests

The sample with flat surface was cut into cuboid (length × width × height was $5 \times 5 \times 6\ mm^3$). The static water contact angle was tested via the sessile drop method using a contact angle meter (Powereach JC2000D4).

2.3.5 Uniaxial compression test

Mechanical properties of aerogels were investigated by a material tester (WDW-2). For the uniaxial compression test, the monolithic aerogel samples were cut into cuboid (length × width × height was $10 \times 10 \times 6\ mm^3$), then compressed under a load cell of 5 kN in a rate of 0.5 mm min^{-1}.

2.3.6 Porous properties tests

The bulk density (ρ_b) was calculated by measuring the mass and volume of aerogel. The skeleton density (ρ_s) was measured by a glass pycnometry (10 ml) in water bath of 25 °C and the porosity (P) was calculated from Eq. 1. All reported values were the means of three replicates.

$$P = \left(1 - \frac{\rho_b}{\rho_s}\right) \times 100\% \quad (1)$$

2.3.7 Oil absorption capacity tests

The oil absorbency of aerogels was characterized by the mass of absorbed oil or organic solvent for per kilogram of aerogel. The aerogel was put into the beaker with organic solvent and taken out when adsorption equilibrium was reached. Then the excess liquid on the surface of aerogels was removed using filter paper and the wet gel was weighed quickly. Three samples for each organic liquid were tested for reproducibility. The absorbency of aerogels could be calculated with the Eq. 2.

$$\Phi = \frac{(m_w - m)}{m} \quad (2)$$

Where Φ was the oil absorbency of aerogels, m_w and m were the mass of wet gels and dry aerogels, respectively.

2.3.8 Absorption and desorption kinetics tests

The absorption and desorption kinetics were tested by the absorption capacity in a certain time interval (3 min for absorption and 10 min for desorption) under room temperature. The aerogels and wet gels were weighed, and then the absorption capacity of absorbed organic solvents was calculated according to Eq. 2.

2.3.9 Recyclability

Successive absorption-desorption process was carried out. In one recycle, aerogel was put into the beaker with solvents ready to be absorbed by aerogel and taken out when adsorption equilibrium was reached. Then the excess liquid on the surface of aerogels was removed using filter paper and the wet gel was weighed quickly. Desorption process was accomplished by evaporation of the solvents at room temperature overnight. After desorption process finished, the dry gel was used for the next absorption. Three samples were tested for reproducibility.

3 Results and discussion

3.1 Preparation and chemical structure of Gelatin-silica aerogels

Monolithic, hydrophobic gelatin-silica composite aerogels were prepared in the current study. The preparation process was shown as Fig. 1. The ethoxyl of TEOS was hydrolyzed into hydroxyl and ethanol firstly. The by-product ethanol promoted the mixture of untreated TEOS and gelatin solution. Part of the hydroxyl groups participated the interaction with gelatin. At the same time, gelatin could form nanofibrous scaffold-like structure by crosslinking [39]. In order to improve the hydrophobicity of composite aerogels, hydrophobic modification was carried out. The gel was soaked with modifier and thermal chemical vapor deposition was employed. During the modification process, the residual hydroxyl groups were replaced by methyl groups.

Successful preparation of gelatin-silica aerogels and hydrophobic modification were confirmed by FTIR analysis (Fig. 2) and scanning electron microscope (SEM) images (Fig. S1). For the pristine gelatin, the wide peaks at 3551 cm^{-1} was attributed to stretching vibration of N–H. The peaks at 1661, 1535, and 1232 cm^{-1} were characteristic absorption peaks of amide I, amide II, and amide III. [37, 40] For the pure silica aerogels, the peak at 1080 and 803 cm^{-1} belonged to asymmetric and symmetric stretching

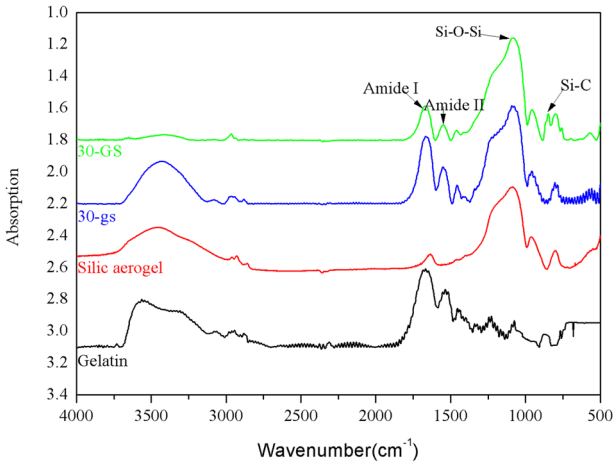

Fig. 2 FTIR spectra of pristine gelatin, silica aerogel, sample 30-gs (unmodified aerogel) and 30-GS (hydrophobic modified aerogel)

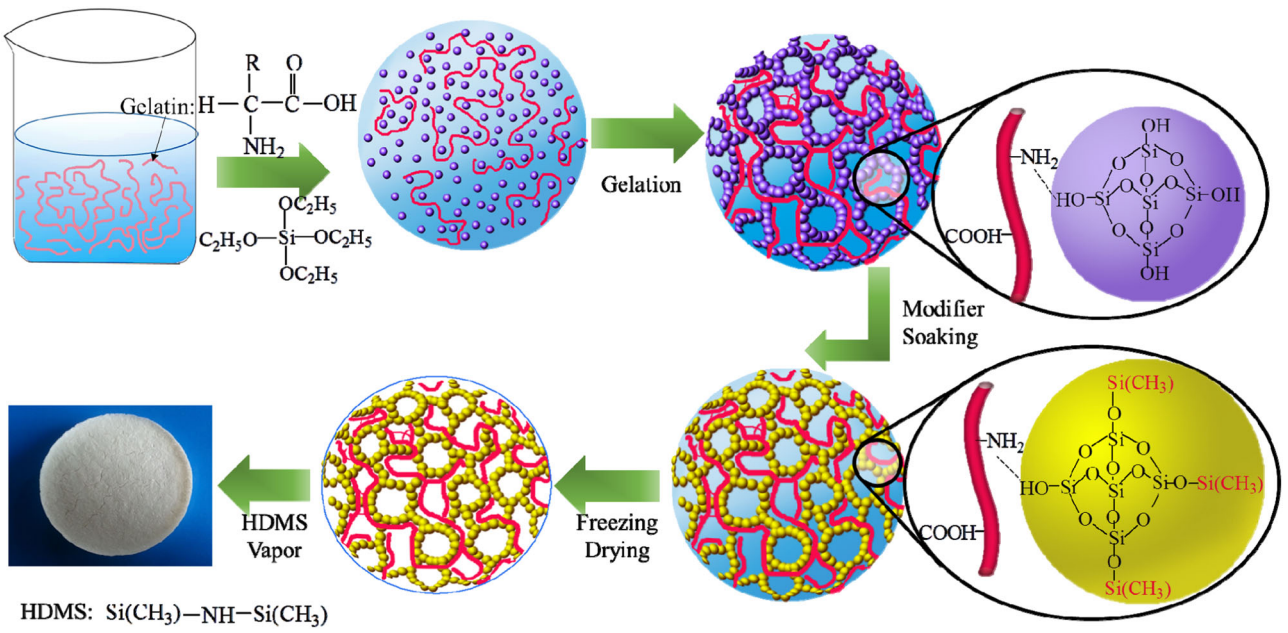

Fig. 1 The preparation scheme of hydrophobic silica–gelatin composite aerogels

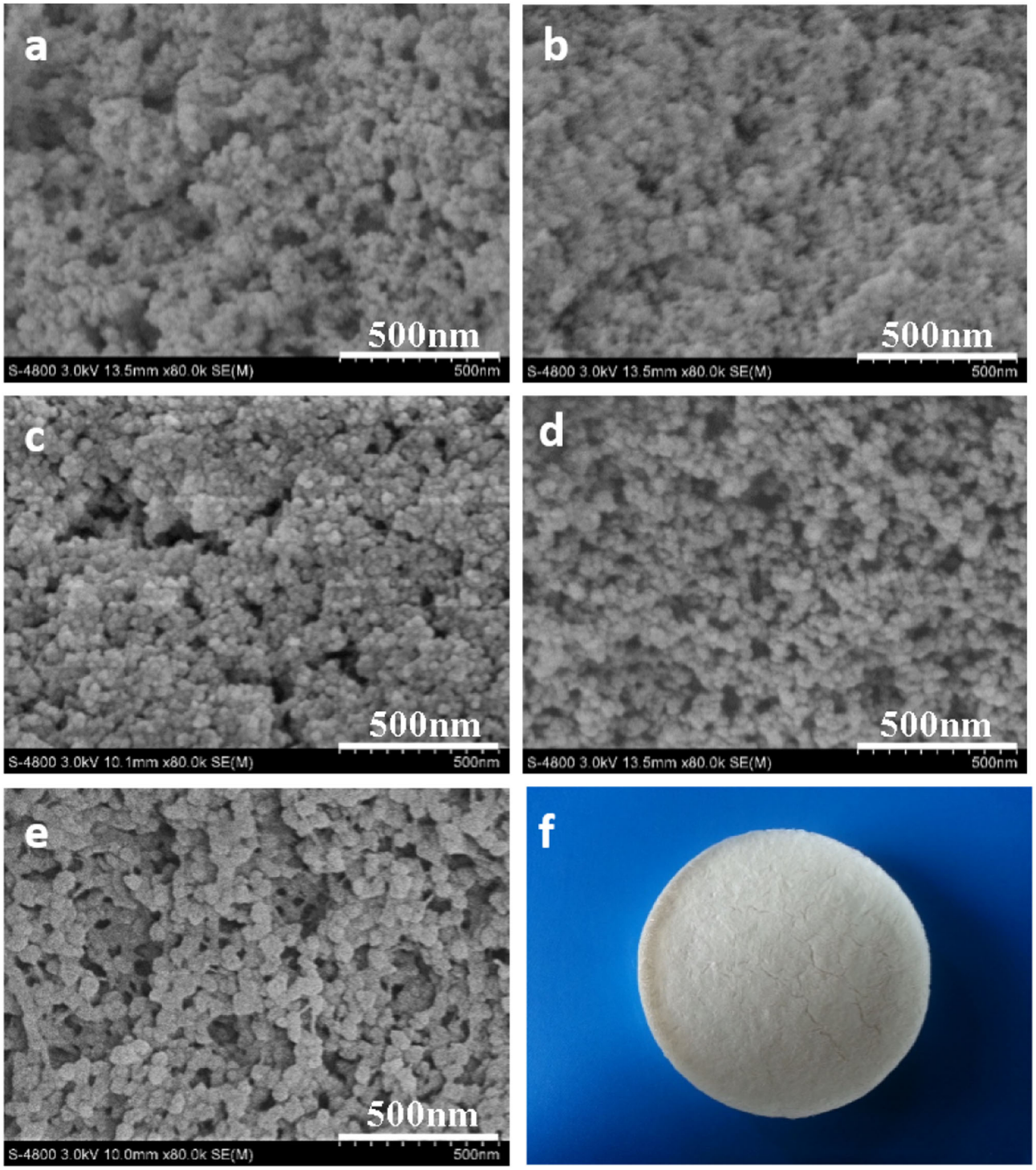

Fig. 3 SEM images of aerogels with different gelatin contents: **a** 0-GS; **b** 10-GS; **c** 20-GS; **d** 30-GS; **e** 40-GS; **f** photo of sample 40-GS

vibration of Si–O–Si, and the peak at 955 cm^{-1} was the stretching vibration of free Si–OH groups [41, 42]. The characteristic absorption peaks of gelatin-silica composite aerogel were accordant with gelatin and silica aerogels and there was no new absorption peak, which might indicate that no covalent bonds except for hydrogen bond formed [43]. In addition, the appearance of absorption peaks of the stretching vibration of Si–C at 849 cm^{-1} in hydrophobic composite aerogels 30-GS suggested the success of modification [41, 43]. For the hydrophobic aerogels, looser network structure and rougher surface were formed compared with unmodified aerogels

(Fig. S1). This may result from the reduced capillary pressure by hydrophobic surface through lowering surface tension, thus leading to the decrease of shrinkage when freeze-drying [41].

3.2 Porous properties of gelatin–silica aerogels

Gelatin contents affected the macro and micro structure of composite aerogels significantly (Fig. S2, 3). When gelatin contents were less than 20%, the aerogels were cracked (Fig. S2). The monolithic aerogels and fine networks were formed when gelatin contents were more than 30%. This might be because when the mass percentage of gelatin was higher than 0.3, the interaction between molecules was strong enough to bear the capillary force during drying process, thus hindering structure collapses and form fine network structures. The SEM of samples (Fig. 3) showed the silica particles were uniformly coated by gelatin. The fine network structures and larger pores were formed with the increase of gelatin contents. It is worthy to note that 40-GS exhibited interconnected network structures composed of gelatin fibers [39] and silica particles (Fig. 3e). This indicated that when the mass percentage of gelatin reached 0.4, the residual gelatin which didn't interact with silica particles formed fibers thus reinforcing the interconnection between the networks. The basic properties of the obtained aerogels, such as density, porosity, and pore volume were shown in Table 1. The bulk density, porosity and pore volume were in the range of 0.068–0.168 g/cm^3, 80–96% and 0.72–1.24 cm^3/g, respectively. The porous property variation trends were accordant with that of SEM images.

3.3 Mechanical properties

Changes of compression resistance property were shown in Fig. 4. 0-GS was unable to bear any loads. 10-GS and 20-GS were cracked (Fig. S2) and their load capacities were similar with 0-GS. 30-GS was broken down when loaded with 20 g. It was noteworthy that negligible deformation was observed for 40-GS when the load was 100 g. The area of the tested aerogel was 0.64 cm^2, thus the composite aerogel of 1 m^2 could support pressure of 1.56×10^4 N. In order to further characterize the mechanical properties, the uniaxial compression tests of 30-GS and 40-GS were carried out. Stress-strain curves of 30-GS and 40-GS exhibited liner elastic reigns, as shown in Fig. 4(2). The Young's modulus of 30-GS and 40-GS were 0.5 MPa and 2.6 MPa, respectively. The strength difference was mainly caused by the changes of network structures. Just as shown in SEM images (Fig. 3), gelatin fibers between network structures were observed in 40-GS. These gelatin fibers enhanced the interconnection between networks, thus higher load force could be borne. Interpenetrating gelatin/alginate composite aerogel was reported by Baldino et al. [39]. The scaffold morphology changed from nanoporous to nanofibrous when gelatin contents were increased. At the same time, Young modulus increased with the increasing of gelatin contents. The result suggested the similar reinforce effect on silica aerogels. The Young's modulus of 40-GS with the low density of 0.096 g/cm^3 was comparable with those of the synthetic polymer reinforced silica aerogel such as polyurethane reinforced silica aerogels (2.5 MPa with density of 0.126 g/cm^3) [44], and resorcinol/formaldehyde cross-linked silica aerogels (2.4 MPa with density of 0.16 g/cm^3) [23].

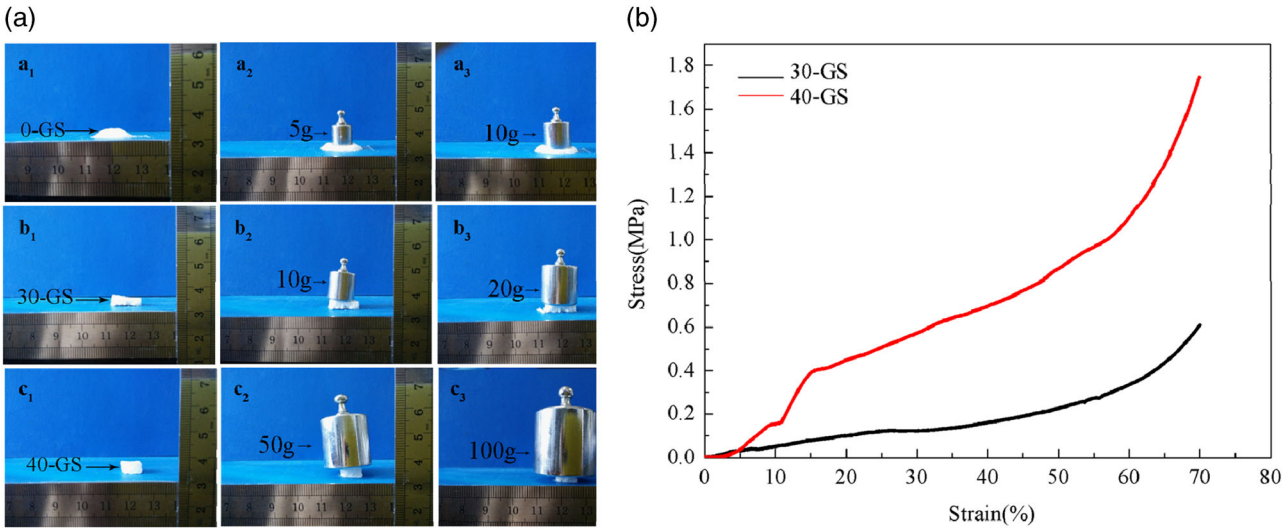

Fig. 4 Compression resistance property of aerogels: **a** The load capacity of 0-GS, 30-GS and 40-GS; **b** uniaxial compression stress-strain curves of 30-GS and 40-GS

3.4 Thermal stability

The thermal stability of gelatin, pure silica aerogel and hydrophobic silica-gelatin composite aerogels with different gelatin contents was measured by a TG analyzer (Fig. 5). The weight losses at 100 °C were associated with the evaporation of residual moisture, and the weight losses at 250–300 °C were attributed to the decomposition of gelatin in composite aerogels [40]. Thermal decomposition temperatures of composite aerogels were higher than 300 °C.

3.5 Surface properties and oil/solvent absorption capacity

The water contact angle of 30-GS was 117° (Fig. 6c). The hydrophobic surface of hydrophobic composite aerogels reduced water adsorption so that the pore collapse was avoided. Thus the stability of the hydrophobic treated composite aerogels in air was improved. The hydrophobic composite aerogels could float on the water. When the beaker was overturned, the hydrophobic composite aerogels passed through water, showing good hydrophobicity (Fig. 6a, b). When the hydrophobic composite aerogel was put into the water/oil mixture, it stayed in oil and was completely wetted, suggesting excellent oil–water selectivity (Fig. 6d).The hydrophobicity and lipophilicity indicated the composite aerogels could be used in the field of oil absorption or oil–water separation application.

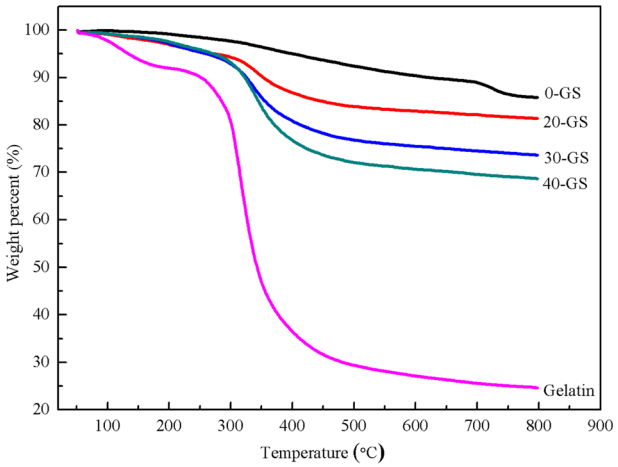

Fig. 5 TG analysis of 0-GS, 20-GS, 30-GS, 40-GS and gelatin

As enormous losses are caused by oil containment leaks, disposement of oil or organic solvents has attracted great interests among researchers and society. The present study investigated the potential application of gelatin-silica composite aerogels in the field of oil or solvents absorption.

Oil or solvent absorption capacity of composite aerogels with different gelatin contents was shown in Table 2. Firstly, for the aerogels with the same gelatin contents, oil/solvents absorption amounts increased with the increase of interfacial tension for all different organic solvents [45] or oils. Secondly, for the same oil/solvents, the change of mass percentage of gelatin in aerogels also led to the change of absorption capacity. According to Eq. 3, absorption power consists of two parts: the capillary force caused by the porous structure and the solvation of solvents [11, 46].

$$2\pi r\gamma\cos\theta = mg \tag{3}$$

where r, γ, and m were radius of pore, interfacial tension, and mass of absorbed solvents or oils, respectively. For the liquids that completely wet the surface, the contact angle θ is zero. Thus Eq. 3 was changed into:

$$2\pi r\gamma = mg \tag{4}$$

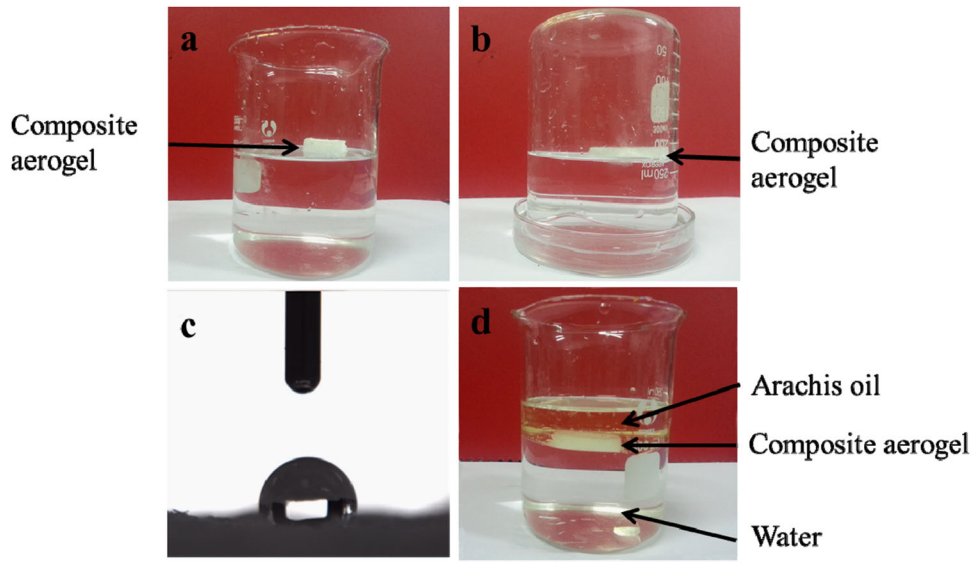

Fig. 6 The hydrophobicity of aerogel: **a** sample 30-GS floated on the water; **b** it passed through water; **c** water contact angle test showed hydrophobicity; **d** aerogel stayed in oil, showing oil–water selectivity

It indicated that absorption capacity increased with the increase of interfacial tension of solvents. Pore property, which mainly depended on the mass percentage of gelatin, affected absorption capacity as well. Larger pore volume could result in the hold of more mass organic liquids. Just as shown in Fig. 7a, absorption capacity for three organic liquids increased with pore volume of composite aerogels. In general, the absorption capacity ranged from 12 to 27

Table 2 Absorption capacity of aerogels with different gelatin contents for different oils/solvents at 20 °C

Organic solvents/oil	Surface tension	Φ (*g*/*g*)			
	(mN/m)	10-GS	20-GS	30-GS	40-GS
Xylene	29.0	19.7 ± 0.7	23.2 ± 0.4	27.0 ± 0.5	19.2 ± 0.4
Methylbenzene	28.5	16.7 ± 0.5	20.6 ± 0.4	25.9 ± 0.6	22.0 ± 0.3
Dichloromethane	27.8	17.0 ± 0.2	20.3 ± 0.3	24.7 ± 0.3	21.4 ± 0.5
Gasoline	–	16.1 ± 0.4	19.3 ± 0.7	22.9 ± 0.4	20.3 ± 0.6
Butyl acetate	25.4	13.9 ± 0.2	17.4 ± 0.8	21.5 ± 0.5	18.2 ± 0.3
Acetone	26.0	11.5 ± 0.4	15.4 ± 0.3	19.7 ± 0.6	16.3 ± 0.4
Arachis oil	–	9.5 ± 0.5	12.6 ± 0.6	16.8 ± 0.3	14.2 ± 0.6
n-Hexane	18.4	8.7 ± 0.6	11.6 ± 0.4	15.1 ± 0.8	14.7 ± 0.6
n-Pentane	16.1	6.9 ± 0.3	8.3 ± 0.6	12.4 ± 0.3	11.4 ± 0.5

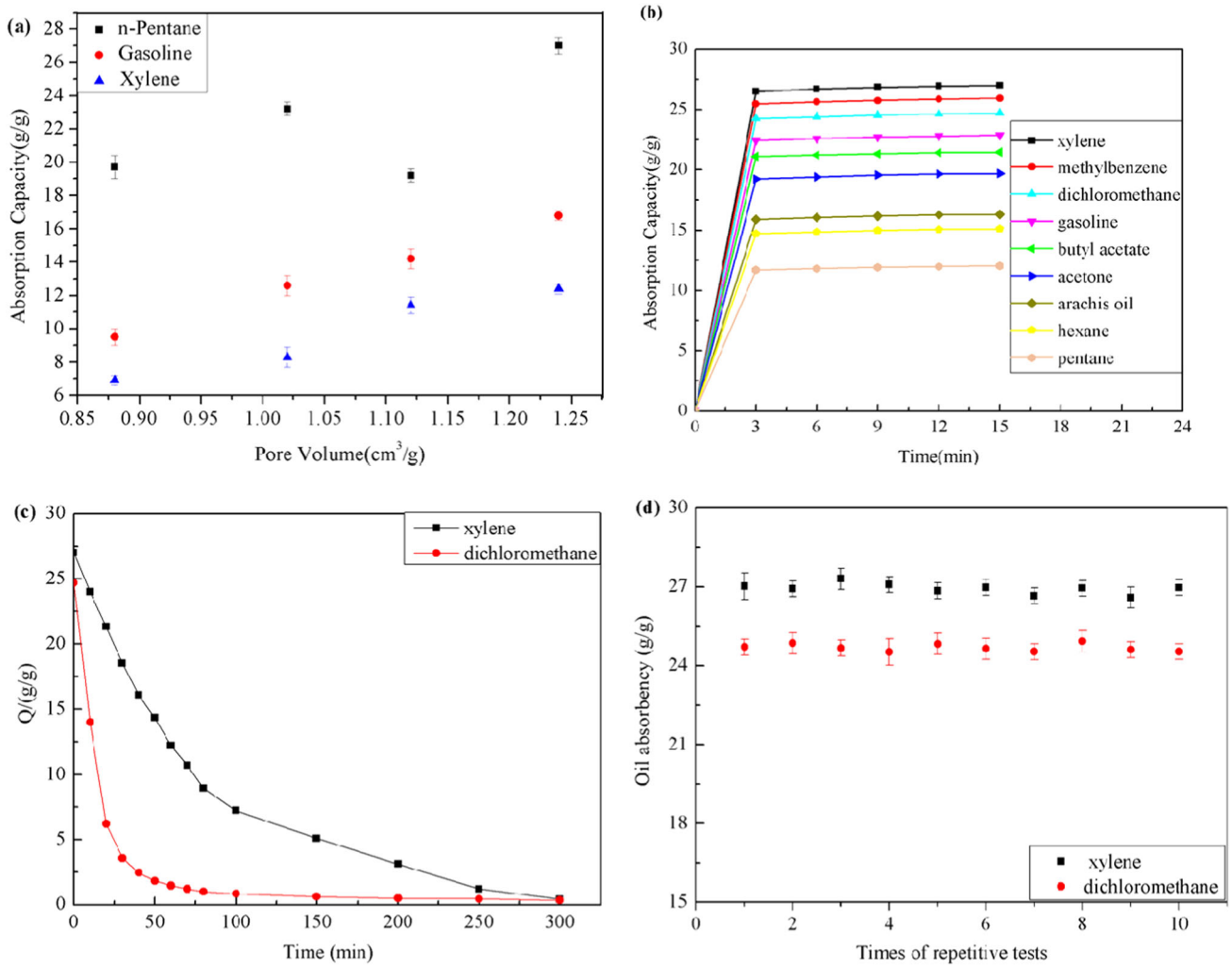

Fig. 7 Oil absorption properties of composite aerogels: **a** Pore volume, depended on gelatin contents, affected absorption capacity. **b** The oil/organic solvents absorption kinetics of 30-GS. **c** Desorption kinetics of 30-GS for xylen and dichloromethane. **d** Recyclability of 30-GS for xylene and dichloromethane

times of its own weight, which was higher than that of the bridged silsesquioxane aerogels (5.1–11.4 times) [21] and silica aerogel microspheres (6.42–12 times) [46].

The absorption, desorption kinetic and recyclability of 30-GS were studied (Fig. 7b–d). The absorption process for all the organic solvents reached equilibrium in 3 min. The fast absorption performance would be encouraging in practical applications. The desorption process occurred through solvents evaporation. The rate of desorption decreased with the increase of interfacial tension. This was due to the desorption process of two stages: Firstly, molecules moved from the interior to the surface through overcoming the interfacial tension effect. Secondly, they were evaporated from the surface depending on the vapor pressure [11]. So the lower the interfacial tension was, the higher the desorption rate was. The successive absorption–evaporation for xylene and dichloromethane was carried out to evaluate the recyclability of gelatin–silica aerogels. The result showed that 30-GS could be reused for more than 10 times and oil absorption capacity slightly decreased (Fig. 7d). The excellent oil/solvent absorption capacity and recyclability indicated the promising application in the fields of oil absorption.

4 Conclusions

In summary, monolithic and hydrophobic biopolymer reinforced silica aerogels with low density were prepared through a simple procedure involving sol–gel method, modifier soaking and freeze-drying as well as chemical vapor deposition of hexamethyl-disilazane. Gelatin contents in the composite aerogels had significant effects on pore structure, mechanical properties and adsorption of oil or organic solvents. With the increase of gelatin contents, the bulk density, porosity, pore volume and oil/organic solvents absorption capacity showed a trend of increase first and then decrease. The composite aerogels 30-GS showed the lowest bulk density (0.068 g/cm^3), the highest porosity (96%), the largest pore (1.25 cm^3/g) and the maximum oil/organic solvents absorption capacity (12–27g/g). The mechanical property was improved due to the increase of gelatin contents. And the Young's modulus reached 2.6 MPa. The excellent oil/solvent absorption capacity, fast absorption kinetics and good recyclability indicated the hydrophobic gelatin-silica composite aerogels could be a promising candidate for oil absorption materials.

Acknowledgements The authors acknowledged the financial support of Science and Technology Foundation of Tianjin (Grants No. 14JCTPJC00505).

Conflict of interest The authors declare that they have no competing interests.

References

1. Xue Z, Cao Y, Liu N, Feng L, Jiang L (2014) J Mater Chem A 2:2445–2460
2. Korhonen JT, Kettunen M, Ras RHA, Ikkala O (2011) ACS Appl Mater Interfaces 3:1813–1816
3. Shannon MA, Bohn PW, Elimelech M, Georgiadis JG, Marinas BJ, Mayes AM (2008) Nature 452:301–310
4. Maleki H (2016) Chem Eng J 300:98–118
5. Husseien M, Amer AA, El-Maghraby A, Taha NA (2009) Int J Environ Sci Tech 6:123–130
6. Ibrahim S, Wang S, Ang HM (2010) Biochem Eng J 49:78–83
7. Adebajo MO, Frost RL, Kloprogge JT, Carmody O, Kokot S (2003) J Porous Mater 10:159–170
8. Chen J, Fang P, Du Y, Hou X (2016) Colloid Polym Sci 294:119–125
9. Du Y, Fang P, Chen J, Hou X (2016) Polym Adv Technol 27:393–403
10. Gurav JL, Rao AV, Nadargi DY, Park HH (2010) J Mater Sci 45:503–510
11. Rao AV, Hegde ND, Hirashima H (2007) J Colloid Interf Sci 305:124–132
12. Yu Y, Wu X, Guo D, Fang J (2014) J Mater Sci 49:7715–7722
13. He S, Huang D, Bi H, Li Z, Yang H, Cheng X (2015) J Non-Cryst Solids 410:58–64
14. Parale VG, Mahadik DB, Kavale MS, Rao AV, Wagh PB, Gupta SC (2011) Soft Nanosci Lett 1:97–104
15. Zhang G, Dass A, Rawashdeh A-MM, Thomas J, Counsil JA, Sotiriou-Leventis C, Fabrizio EF, Ilhan F, Vassilaras P, Scheiman D, McCorkle L, Palczer A, Johnston JC, Meador MA, Leventis NJ (2004) J Non-Cryst Solids 350:152–164
16. Shahzaman M, Bagheri R, Masoomi M (2016) J Non-Cryst Solids 452:325–335
17. Matias T, Varino C, de Sousa HC, Braga MEM, Portugal A, Coelho JFJ, Duraes L (2016) J Mater Sci 51:6781–6792
18. Domenech B, Mata I, Molins E (2016) RSC Advances 6:10736–10742
19. Zhang Y, Wang J, Wei Y, Zhang X (2017) New J Chen 41:1953–1958
20. Wang X, Jana SC (2013) ACS Appl Mater Interfaces 5:6423–6429
21. Wei Y, Wang J, Zhang Y, Wang L, Zhang X (2015) RSC Adv 5:91407–91413
22. Wang Z, Wang D, Qian Z, Guo J, Dong H, Zhao N, Xu J (2015) ACS Appl Mater Interfaces 7:2016–2024
23. Yun S, Luo H, Gao Y (2015) J Mater Chem A 3:3390–3398
24. Ma Q, Liu Y, Dong Z, Wang J, Hou X (2015) J Appl Polym Sci 132(41770):1–11
25. Yun S, Luo H, Gao Y (2014) J Mater Chem A 2:14542–14549
26. Sai H, Xing L, Xiang J, Cui L, Jiao J, Zhao C, Li Z, Li F (2013) J Mater Chem 1:7963–7970
27. Visser J, Gawlitta D, Benders KEM, Pouran SMH, van Weeren PR, Dhert WJA, Malda J (2015) Biomaterials 37:174–182
28. Duconseille A, Astruc T, Quintana N, Meersman F, Sante-Lhoutellier V (2015) Food Hydrocollodis 43:360–376
29. Alfaro AT, Balbinot E, Weber CI, Tonial IB, Machado-Lunkes A (2015) Food Eng Rev 7:33–44
30. Negahi Shirazi A, Fathi A, Suarez FG, Wang Y, Maitz PK, Dehghani FA (2015) ACS Appl Mater Interfaces 8:1676–1686
31. Veres P, Keri M, Banyai I, Fabian I, Domingo C, Kalmar J (2017) Colloids and Surfaces B: Biointerfaces 152:229–237
32. Mahony O, Tsigkou O, Lonescu C, Minelli C, Ling L, Hanly R, Smith ME, Stevens MM, Jones JR (2010) Adv Funct Mater 20:3835–3845
33. Arcos D, Vallet-Regí M (2010) Acta Biomater 6:2874–2888

34. Mahesh S, Joshi SC (2015) Int J Heat Mass Transfer 87:606–615
35. Veresa P, López-Periago AM, Lázár I, Saurina J, Domingo C (2015) Int J Pharmaceutics 496:360–370
36. Lei B, Shin KH, Noh DY, Jo IH, Koh YH, Choib WY, Kimb HE (2012) J Mater Chem 22:14133–14140
37. Dashnyam K, Perez RA, Singh RK, Lee E-J, Kim H-W (2014) RSC Advances 4:40841–40851
38. Wang A, Yang Y, Yan X, MaG, Bai S, Li J (2016) RSC Advances 6:70064–70071
39. Baldino L, Concilio S, Cardea S, Reverchon E (2016) Polymer 8:1–12
40. Frazier SD, Srubar III WV (2016) Mater Sci Eng C 62:467–473
41. Jeong AY, Koo SM, Kim DP (2000) J Sol–Gel Sci Technol 19:483–487
42. Wang J, Zhou Q, Song D, Qi B, Zhang Y, Shao Y, Shao Z (2015) J Sol–Gel Sci Technol 76:501–509
43. Yang L, Guo J, Yu Y, An Q, Wang L, Li S, Huang X, Mu S, Qi S (2016) Carbohydr Polym 142:275–281
44. Duan Y, Jana SC, Lama B, Espe MP (2013) Langmuir 29:6156–6165
45. Jasper JJ (1972) J Phys Chem Ref Data 1:841–1010
46. Yun S, Luo H, Gao Y (2014) RSC Adv 4:4535–4542